J Mater Sci: Mater Med (2013) 24:1627–1637
DOI 10.1007/s10856-013-4920-7

Premixed injectable calcium phosphate cement with excellent suspension stability

Fangping Chen · Yuhao Mao · Changsheng Liu

Received: 21 November 2012 / Accepted: 18 March 2013 / Published online: 6 April 2013

Abstract Premixed injectable calcium phosphate cement (p-ICPC) pastes have advantages over aqueous injectable calcium phosphate cement (a-ICPC) because p-ICPC remain stable during storage and harden only after placement into the defect. This paper focused on the suspension stability of p-ICPC paste by using fumed silica as a stabilizing agent and propylene glycol (PEG) as a continuous phase. Multiple light scanning techniques were first applied to evaluate the suspension stability. The results indicated that fumed silica effectively enhanced the suspension stability of p-ICPC pastes. The stabilizing effect of fumed silica results from the network structure formed in PEG because of its thixotropy. The p-ICPC could be eventually hydrated to form hydroxyapatite under aqueous circumstances by the unique replacement between water and PEG. p-ICPC (1) not only possesses proper thixotropy and compressive strength but has good injectability as well. p-ICPC (1) was cytocompatible and had no adverse effect on the attachment and proliferation of MG-63 cells in vitro. These observations may have applicability to the development of other nonaqueous injectable biomaterials for non-immediate filling and long-term storage.

F. Chen · C. Liu
The State Key Laboratory of Bioreactor Engineering, East China University of Science and Technology, Shanghai 200237, People's Republic of China

F. Chen (✉) · C. Liu (✉)
Key Laboratory for Ultrafine Materials of Ministry of Education, School of Materials Science and Engineering, East China University of Science and Technology, Meilong Road 130, P.O. 112#, Shanghai 200237, People's Republic of China
e-mail: chenfangping06@yahoo.com.cn

C. Liu
e-mail: liucs@ecust.edu.cn

Y. Mao
Engineering Research Center for Biomedical Materials of Ministry of Education, East China University of Science and Technology, Shanghai 200237, People's Republic of China

1 Introduction

Bone fractures in the elderly, mainly resulting from osteoporosis, have recently seen a marked increase in frequency and severity. As the population ages the need to repair the bone defect is increasing dramatically [1]. The scope of minimally invasive surgery is constantly expanding. With the advance in instrumentation and surgical skill, the directly injectable biomaterials are allowed to be implanted into the defect through smaller incisions.

Aqueous injectable calcium phosphate cement (a-ICPC), taking a variety of aqueous media (e.g. distilled water, phosphate-buffered saline solution, sodium phosphate + citric acid aqueous solution) as setting liquid, has proved to be an alternative bone substitute with great clinical convenience [2]. a-ICPC has combined characteristics of biocompatibility, osteoconductivity, in situ setting and easy shaping for any complicated contours of bone defect [3]. It is worthwhile to note that the a-ICPC has to be prepared just before implantation, since setting starts from the moment that the powder comes in contact with water.

However, it is not only difficult for the clinician to mix the powder with liquid thoroughly, but hard to inject the a-ICPC into the defect within a prescribed time as well. In addition, the operation of on-site powder-liquid mixing prolongs the surgical time. It may compromise the implant performance because of inhomogeneous mixing and insufficient filling stemming from the limited mixing time [4]. These prompted the development of premixed injectable calcium phosphate cement (p-ICPC) [5].

The p-ICPC, taking nonaqueous but water-miscible liquid as liquid phase, is stable and does not harden in storage or in a syringe, because calcium phosphate cement (CPC) hardens only when exposed to an aqueous environment. However, mixtures of solid particles suspended in a viscous liquid are ubiquitous in applications. Due to their high density, the suspended particles are prone to gravitational settling upon long-term storage, thus causing a separation of the solid and liquid phases [6]. A more significant problem is that the pure p-ICPC can not resume the original consistency with stimulus removal. This makes p-ICPC difficult to inject at later times because of the reduction of the uniformity of the suspension. In addition, the sedimentation of CPC powders in liquid is apt to prolong the setting time and decrease the injectability. Obviously, the above drawbacks of the p-ICPC, which are mainly relevant to the stability, limit its potential clinical application.

It is well accepted that the expiration date of the commercially available injectable biomaterial is conditioned by the stability of the suspension. In addition, long-term stability of the suspension is one major criterion for the use of such a medical device, since it controls the validity and the required storage conditions of the p-ICPC. Usually, suspension stability is not mentioned in academic papers reporting advances in injectable cement, since the solid is assumed to be mixed with the liquid just before the operation. Although the factors important to control the long-term stability of the β-tricalcium phosphates/monocalcium phosphate monohydrate (β-TCP/MCPM) were investigated [7], the suspension stability and the real possibility to handle the nonaqueous ICPC after a long-term storage are poorly documented. In addition, little attention has been paid to the rheological behavior of the p-ICPC suspension, which is sensitive to the structure recovery of the suspension.

The purposes of this study were (i) to develop a premixed injectable calcium phosphate cement with improved suspension stability via taking viscoplastic media propylene glycol (PEG) as a continuous phase and introducing fumed silica as a thixotropic agent, and (ii) to investigate the suspension stability, rheological properties, injectability, phase composition, microstructure and cytocompatibility in vitro.

2 Materials and methods

2.1 Materials and preparation

The p-ICPC consists of powder and liquid phase. All calcium phosphates used in this experiment were purchased from Shanghai Rebone Biomaterials Ltd., P.R. China. The CPC powder was composed of tetracalcium phosphate [TECP, $Ca_4(PO_4)_2O$] and dicalcium phosphate anhydrous [DCPA, $CaHPO_4$] in an equivalent molar ratio [8, 9]. After being airflow-grinded twice, the CPC powders were then sieved to obtain particles with diameter size ranged from 20–50 μm.

The liquid phases consist of 1,3-propylene glycol (PEG), disodium hydrogen phosphate (Na_2HPO_4) and fumed silica. Because of its water-soluble, nontoxic and biocompatible properties [10], PEG is used as a nonaqueous liquid [4]. For example, PEG is known as a lubricant and has been used in beverage, food, cosmetic and biomedical fields [11, 12]. To shorten the p-ICPC setting time in the aqueous surrounding, 2 wt% anhydrous Na_2HPO_4, a common setting accelerator [13, 14], was introduced into the liquid phase. To improve suspension stability of the paste, fumed silica with 20 nm (Cabot Chemical Co., Ltd., Shanghai, China), as a thixotropic agent, was added to the nonaqueous phase with different contents (1 and 2 wt%) by ultrasonic dispersion for 10 min at 25 °C [15, 16]. The content of fumed silica in liquid phase of p-ICPC was indicated in parentheses. For example, p-ICPC (1) represented p-ICPC paste containing 1 wt% fumed silica in the liquid phase.

The p-ICPCs were prepared by mixing the blended CPC powders with the liquid homogeneously at the fixed powder to liquid (P/L) ratio of 2 g ml^{-1} by a spatula. Pure ICPC without fumed silica [p-ICPC (0)] was used as control. The pastes were quickly packed into flexible plastic tube, tightly sealed to isolate them from moisture and stored in desiccators at room temperature. Notably, as far as the p-ICPC suspension is concerned, the powders in the p-ICPC would not be reacted with the nonaqueous liquid. All the chemicals used in preparation of p-ICPC had a purity level of reagent grade unless otherwise noted.

2.2 Rheological properties

Rheological properties (including viscosity and thixotropy) were used to determine the internal structure of paste, which is related to suspension stability [17]. Rheological measurements of all p-ICPC pastes were conducted by a rotational rheometer (RS600, Thermo Hakke Co., Ltd., USA). After being mixed thoroughly for 3 min, the sample was poured into the geometry of the plate assembly of the rheometer. To avoid undesired influence from different mechanical histories, the samples were allowed to shear at an identical rate of 100 s^{-1} for 20 s to establish a baseline shear history at 37 °C.

The flow curves and hysteresis loops were obtained by registering at controlled rate conditions with a three-stage measuring program with a linear increase of shear rate from 0.08 to 100 s^{-1} in 5 min, a plateau held at 100 s^{-1} for 1 min and a decrease from 100 to 0.08 s^{-1} in 5 min. We chose an initial reference viscosity value for conditions in

which the shear rate was 0.08 s^{-1}. Thixotropy was determined using Rheowin Pro software (Version 2.64, Thermo Hakke Co., Ltd., USA) as the area enclosed between the up-curve and the down-curve in the controlled shear rate range considered above. All the tests were conducted at a constant temperature of 25 °C.

2.3 Injectability and compressive strength

The injectability of p-ICPC was tested according to the same procedure as described before [18]. The powders and the nonaqueous liquid were mixed adequately for 3 min to form pastes and then transferred into a syringe with an inner diameter of 14.5 mm. The syringe is fitted with a needle of 0.7 mm inner diameter for root canal filling, which is much smaller than those used in a-ICPC [19]. A 29.4 KN compressive load at the rate of 0.5 mm min^{-1} was then applied vertically on top of the plunger. The percentage of injectability was calculated by dividing the mass expelled from the syringe by the total amount of cement charged into the syringe in 2 min. Each test was performed three times and the average value was calculated.

The p-ICPC (1) was loaded into a polytetrafluoroethylene (PTFE) mold (Φ6 × 10 mm) with a spatula, which was immersed in deionized water and kept in a 100 % relative humidity environment at 37 °C. After 6 h, samples were removed from the mold and immersed in deionized water further for 66 h. The p-ICPC (0) was placed into PTFE and then stored in a 100 % relative humidity environment at 37 °C for three days. Before testing, the hardened samples were uniformly polished on both sides. The compressive strength of the cement was measured at a loading rate of 1 mm min^{-1} using a universal testing machine (AG-2000A, Shimadzu Co. Ltd., Japan). Three replicates were carried out for each group, and the results were expressed as mean ± standard deviation (mean ± SD).

2.4 Suspension stability assessment

Suspension stability of p-ICPC was evaluated by a concentrated liquid dispersion (Turbiscan LA-b ^{Expert}, Formulation Co., Ltd., France). The dispersion is placed in a cylindrical glass cell and scanned from bottom to top with a pulsed near-infrared light source ($\lambda = 850$ nm). The detection head is composed of two synchronous transmission (T) and back scattering (BS) detectors. T detector received the light going through the sample (180 = from the incident light), and BS detector received the light scattered backward by the sample (45 = from the incident light) along the height of the cell [20]. The turbiscan works in a scanning mode: the optical reading head scans the length of the sample acquiring transmission and backscattering data every 40 μm. The corresponding curves provide the transmitted and backscattered light flux as a function of the sample height (in mm). Scans are repeated over time, each one providing a curve, and all curves are overlaid on one graph to show stability over time. Therefore, the T and BS profiles contain overall (sedimentation and aggregation) kinetics information and the relative migration speed of the particles.

2.5 Phase analysis and microstructure observation

Simulated body fluid (SBF) was prepared as follow: reagent-grade sodium chloride (NaCl, 7.996 g), sodium hydrogen carbonate ($NaHCO_3$, 0.353 g), potassium chloride (KCl, 0.224 g), potassium hydrogen phosphate ($K_2HPO_4{\cdot}3H_2O$, 0.228 g), six hexahydrate magnesium chloride ($MgCl_2{\cdot}6H_2O$, 0.305 g), hydrochloric acid (HCl, 0.045 mol), calcium chloride ($CaCl_2$, 0.278 g), sodium sulfate (Na_2SO_4, 0.071 g) and trihydroxymethy laminomethane (Tris, 6.057 g) were in order dissolved in deionized water to form 1L SBF. To prepare clear SBF with no precipitation, only when the previous reagent has been dissolved completely, can the succedent reagent be added to the solution. The solution was then buffered to pH 7.4 at 37 °C with Tris or HCl. The ion concentrations and pH of the SBF are similar to those in human blood plasma.

The p-ICPCs were loaded into a PTFE mold (Φ6 × 10 mm) with a spatula, which was immersed in SBF kept in a 100 % relative humidity environment at 37 °C. After 6 h, samples were removed from the mold and immersed in SBF in a shaking water bath at 37 °C with a surface area-to-volume ratio of 0.5 cm^{-1} [21]. The p-ICPC was soaked in SBF for 1, 3, 7 and 11 days respectively, and the solution was changed every day. At the predefined soaking time, the samples were gently rinsed with deionized water to remove SBF immediately, and immersed in liquid nitrogen for 15 min to stop the setting reaction, then dried at 37 °C over night. The samples were milled in a mortar and the phase composition were examined by X-ray diffraction (XRD, D/max 2550 VB/PC, Rigaku Co., Japan) with Cu K_α radiation and Ni filter ($\lambda = 1.5406$ A, 100 mA, 40 kV) in a continuous scan mode. The diffraction data were collected from 10 to 75°, with a step size of 0.02° at a scan speed of 10 min^{-1}.

Samples with different soaking time were sputter-coated with gold- palladium with 20 nm thickness. Scanning electronic microscopy (SEM, JSM-6360LV, Jeol, Japan) was used to examine the microstructure of the resultant p-ICPC.

2.6 Cytocompatibility in vitro

Cell culture was performed to evaluate the cytocompatibility of the cements in vitro. MG-63 osteoblast-like cells

were cultured in Dulbecco's modified Eagle's medium (DMEM) supplemented with 10 % volume fraction of fetal bovine serum (FBS), 1 % L-glutamine, 100 U ml^{-1} penicillin and 100 μg ml^{-1} streptomycin at 37 °C in a humid atmosphere of 5 % CO_2 in air. The culture medium was refreshed every two days.

The proliferation of MG-63 cells cultured on the samples was assessed quantitatively using methyl thiazoly tetrazolium (MTT) assay. The p-ICPC (1) and p-ICPC (0) discs, with the size of 5 mm in diameter and 2 mm in thickness, were prepared as the method described in Sec. 2.3. The samples were sterilized by ethylene oxide gas. Tissue culture polystyrene (TCP) was selected as a control. MG-63 cells with a density of 5×10^3 cells per disc were seeded evenly into the wells with a pipette, followed by incubation in a DMEM medium at 37 °C and 100 % humidity with 5 % CO_2 for 1, 3 and 5 days, with the medium replaced every second day. The cell-seeded discs were further incubated for 4 h. Subsequently, the culture medium of each well was removed. The residual cultured medium and unattached cells were removed from the cell-seed discs by washing with PBS three times. After the attached cells on the discs were digested by trypsin, the adherent cells were counted with haemacytometer, and the cell attachment efficiency was determined by counting the cell number remaining in the wells.

Three disc-shaped (Φ10 × 2 mm) p-ICPCs (1) were used to assess the cell morphology on the cement surface. The sterilized samples were put in a 24-well plate. MG-63 cells with a density of 6×10^3 cells per disc were seeded evenly into the wells with a pipette, followed by incubation at 37 °C under 5 % CO_2 condition in DMEM medium. The medium was replaced every 2 days. After culturing for 3 days, the sample-cell constructs were rinsed twice with PBS, fixed with 1 % volume fraction of glutaraldehyde and subjected to graded ethanol dehydrations. The samples were air-dried in desiccators overnight and sputter-coated with gold-palladiumon prior to SEM observation. The morphology of the cells was observed by SEM (JSM6360, JEOL).

3 Results

3.1 Rheological properties

Figure 1 shows the viscosity curves and thixotropic curves of p-ICPC pastes containing different amounts of fumed silica. The rheological parameters including initial viscosity, thixotrop and yield stress of p-ICPC pastes were calculated in Table 1 by using Rheowin Pro software according to Fig. 1. The viscosity of all pastes decreased with the increase of shear rate. The result indicated the addition of fumed silica did not change the shear-thinning characteristic of the p-ICPC, and all p-ICPCs showed pseudoplastic flow behavior. More importantly, the addition of fumed silica improved the initial viscosity of all pastes. When the shear rate decreased from 100 to 0.08 s^{-1}, the viscosity of the pastes returned back to the original value except the p-ICPC (0). Thixotropic curves of the p-ICPC pastes with fumed silica were plotted in Fig. 1b. With the increasing amount of fumed silica, the initial viscosity, the thixotropy and the yield stress of the p-ICPC paste were obviously increased (Table 1).

3.2 Injectability of p-ICPC

Figure 2 displays the influence of fumed silica with different contents on the injectability and compressive strength of the p-ICPC pastes. p-ICPC (0), p-ICPC (0.5), p-ICPC (1), p-ICPC (1.5) and p-ICPC (2) were used to study the injectability. The addition of fumed silica reduced the injectability of p-ICPC pastes obviously. When the content of fumed silica increased from 0 to 1.5 wt%, the injectability dropped from (83.13 ± 3.38) % of p-ICPC (0) to (56.33 ± 3.15) % of p-ICPC (1.5). With further increasing the content of fumed silica to 2 wt%, the injectability of the p-ICPC (2) was significantly reduced to (28.06 ± 2.07) %, which is too low for clinical application. The compressive strength increased as the content of fumed silica increased from 0 to 2 %. Interestingly, p-ICPC (1) not only possesses proper thixotropy and compressive strength but had good injectability as well. It will be expedient for surgeons to inject the p-ICPC (1) to the implant site more easily. Therefore, p-ICPC (1) was selected for the next experiment and p-ICPC (0) was taken as a control.

3.3 Suspension stability of p-ICPC

Figure 3 shows typical transmission and backscattering profiles as function of the sample height obtained in the case of the p-ICPC (0) and p-ICPC (1). The curves represented status of paste at the various scanning time. No variation was found between the curves of transmittance and backscattering for p-ICPC (1). However, significant settling was observed along the whole height of the p-ICPC (0), especially at the top. The result showed that 1 % fumed silica stabilized the injectable calcium phosphate cement suspension effectively.

Turbiscan provided transmittance profiles for p-ICPC during the optical analysis. Figure 4a shows a typical transmission and backscattering profiles as function of time obtained in the case of the p-ICPC (0) and p-ICPC (1). The transmittance variation profiles of p-ICPC (1) seemed to intersect the base line at the same point during the whole scan period. The phenomenon showed the suspension

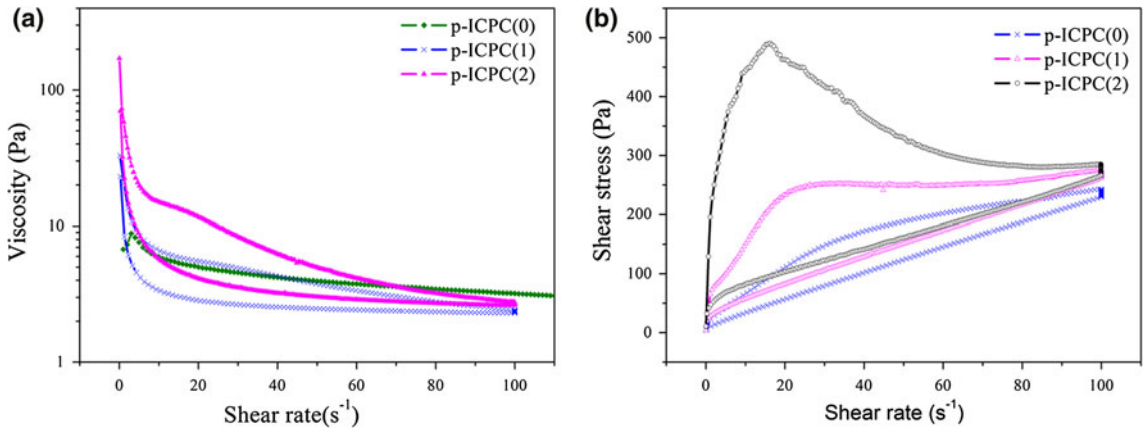

Fig. 1 Viscosity curves **a** and thixotropic curves **b** of p-ICPC pastes with different contents of fumed silica

Table 1 Calculated rheological parameters of p-ICPCs with different contents of fumed silica

Contents of fumed silica (wt%)	Rheological parameters		
	Initial viscosity (Pa·s)	Thixotropy (Pa·s)	Yield stress (MPa)
0	8.84	3227	0
1	33.01	4702	23.65
2	170.98	8590	255.78

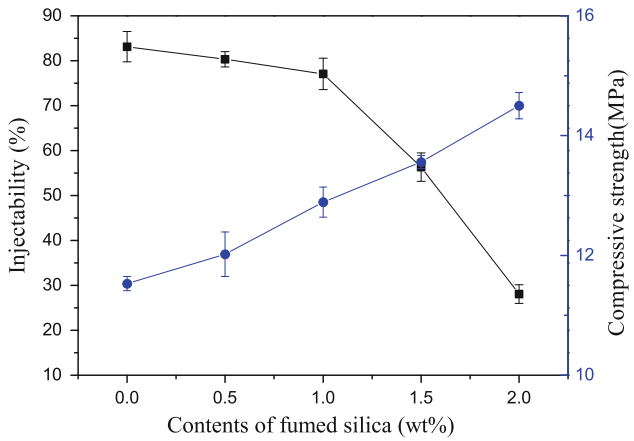

Fig. 2 Influence of the fumed silica content on the injectability and compressive strength of p-ICPC pastes

stability of p-ICPC (1) was improved significantly. The variation of BS signals as a function of time for p-ICPC (0) and p-ICPC (1) are also compared in Fig. 4a. The backscattering variation for p-ICPC (0) reduced 21.2 % after scanning for 5 days. However, the backscattering variation for p-ICPC (1) was decreased by 0.11 % even after scanning for 10 days, indicating that no significant aggregation or sedimentation occurred.

As for the suspension, the longer the sedimentation time the more stable the p-ICPC is. Figure 4b shows the variation of migration rate of solid-phase particles with sedimentation time in p-ICPC. The p-ICPC (1) began sedimentation after 7 days, which is much later than p-ICPC (0) of 2.77 days. During the whole scanning period of 5 days, the particle migration rate of p-ICPC (0) reached 0.27 mm d^{-1}. Notably, even upon storage for 10 days, the particle in p-ICPC (1) sedimented at the rate of 0.03 mm d^{-1}, only one-tenth of that for p-ICPC (0). Obviously, the suspension stability of p-ICPC (1) is better than that for p-ICPC (0), which is in a good agreement with rheological data.

3.4 Phase analysis and microstructure observation

The X-ray diffraction (XRD) patterns of p-ICPC (0) and p-ICPC (1) immersed in SBF for 1, 3, 7 and 11 days are shown in Fig. 5 respectively. As indicated in XRD patterns, the apatite phase is present on all the hydrated p-ICPC surfaces, and the peaks of apatite phase after immersion in SBF for 11 days grew obviously and became sharp. With the increase of the soaking time, the relative intensity of peaks characteristic of TECP crystals decreased. The result revealed the p-ICPC was hydrated in the SBF and converted to hydroxyapatite (HAP) gradually.

Typical scanning electron microscopic photographs of the fracture surface for p-ICPC (1) pastes after soaking in SBF for different periods are shown in Fig. 6. At the same magnification (10,000×), it could be observed that all the p-ICPCs soaked in SBF were constructed by bridged crystalline particles. After one-day immersion in SBF, the needle-like HAP granules are scattered over the surface of p-ICPC (1), with a length of 0.5–1 μm and a diameter of approximately 0.1 μm, being evident in SEM (Fig. 6a). With the immersion time up to 3 days, a large number of needle-like HAP grains were precipitated into a network

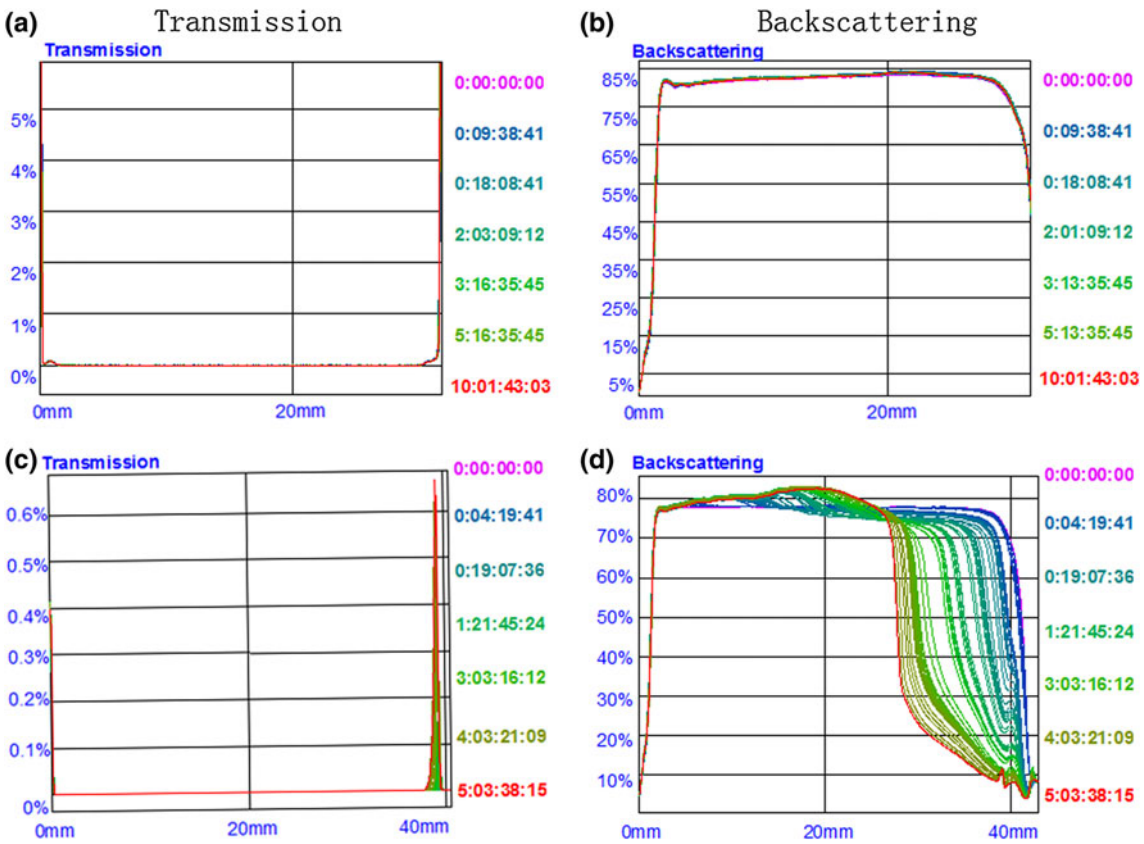

Fig. 3 **a** Transmission light curves of p-ICPC (1) with sample height. **b** Backscattered light curves of p-ICPC (1) with sample height. **c** Transmission light curves of p-ICPC (0) with sample height. **d** Backscattered light curves of p-ICPC (0) with sample height

structure (Fig 6b). In addition, a limited number of the platelet-like hydrated products were located on the fracture surfaces. The platelet-like crystals are 1–2 μm in width and 0.2 μm in thickness. After immersion in SBF for 7 days, the morphology of the hydrated products changed, and a large number of platelet-like crystals replaced the small needle-like crystals. In addition, the platelet-like crystals were tightly interlaced to the network structure (Fig. 6c). After immersion in SBF for 11 days, a certain number of rod-like crystals, with a length of 15–25 μm and a width of approximately 0.5 μm, were found to grow regularly on the fracture surfaces of p-ICPC (1) (Fig. 6d–f).

3.5 Cytocompatibility

In order to observe the cell response to synthetic materials, in vitro studies of cell/substrate interaction are performed. Figure 7 shows the proliferation curves of MG-63 cells on the TCP control, p-ICPC (0) and p-ICPC (1). Obviously, the TCP control had the highest cell density. The cell numbers for both pastes increased with increased incubation time. The number of viable cells on the p-ICPC (1) was not significantly different from the p-ICPC (0). The results reveal that neither p-ICPC (1) nor p-ICPC (0) are cytotoxic.

The morphological feature of MG-63 cells cultured on p-ICPC (1) for 3 days was observed by SEM, shown in Fig 8. The cells were attached to and spread well on the surfaces of both pastes. The cells on the p-ICPC (1) exhibited similar spindle-like morphology and had developed filopodial extensions with lengths up to 50 μm, which are observed to be contacting cells to the substrate and to neighboring cells. This indicates p-ICPC (1) had no negative effects on cell morphology and viability.

4 Discussion

A constraining factor for p-ICPC is subject to phase separation. Generally, it was considered to be kinetically stable if the destabilization rate of the suspension is low enough compared with the expected lifespan. In this study, to avoid phase separation and improve the suspension stability, viscoplastic media PEG as continuous phase and fumed silica as a thixotropic agent were introduced to ICPC paste, thus p-ICPC was prepared by mixing the powder-liquid in advance. Since the suspension stability is related to the size of the particles making up the dispersed phase, the CPC particles used in this study were in the same size.

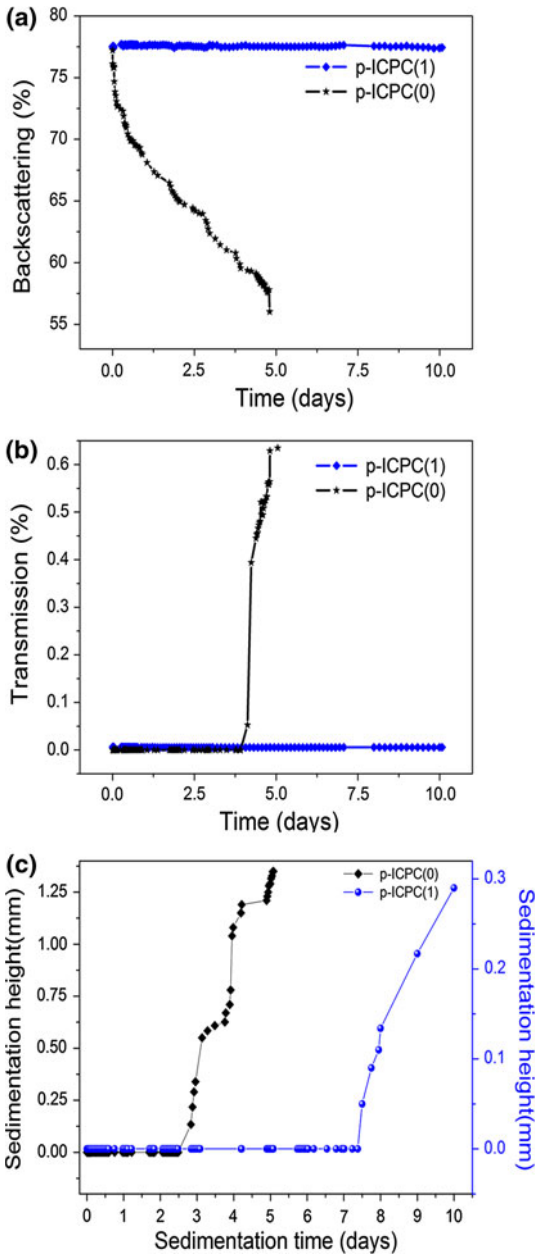

Fig. 4 **a** Backscattered light curves of p-ICPC (0) and p-ICPC (1) with time. **b** Transmitted light variation curves of p-ICPC (0) and p-ICPC (1) with time. **c** Particle migration rate of solid-phase particles in p-ICPC (0) and p-ICPC (1)

Nonaqueous solvents have been more commonly used in suspension because of the enhanced powder dispersion. Rankin et al. [22] proved that the viscoplastic media as a continuous phase was successful in reducing the sedimentation rate of the suspension. PEG, approved by FDA and applied extensively in biomedical fields, was further confirmed to stabilize the suspension system by forming a viscous solution [23]. In this study, PEG was used as a continuous phase to improve the stability of p-ICPC.

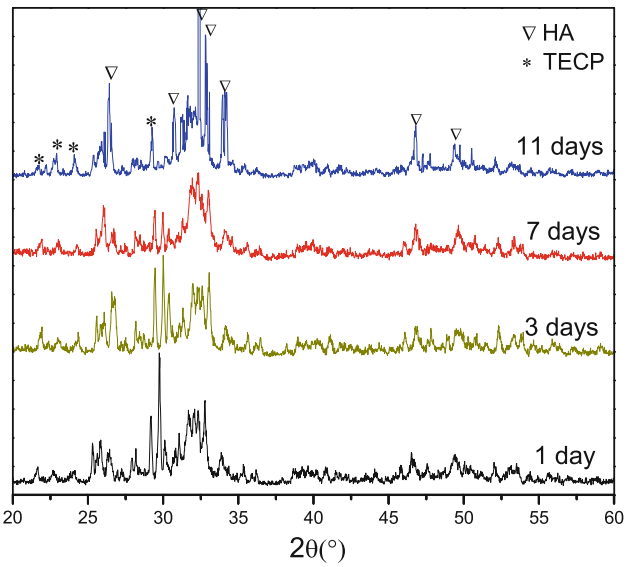

Fig. 5 XRD patterns of p-ICPC (1) after incubation in SBF for 1, 3, 7 and 11 days

The kinetic suspension stability can also be attained by adding thixotropic agents [24–26]. Recently, fumed silica has been successfully used to control the rheology by providing a strong thixotropic effect, which is associated with the build up of 3D network aggregates and gelation [27]. In the study reported here, fumed silica as a thixotropic agent will be incorporated into p-ICPC to improve the suspension stability.

Rheology is an indirect method to determine the stability by providing additional information (viscosity, yield stress and thixotropy loop area) of the suspension. Generally, high viscosity contributes to improving the suspension stability [28]. Thixotropy loop area was used to evaluate the magnitude of thixotropy of the paste during motion, which is proportional to the energy required to break down the thixotropic structure [29]. The larger the thixotropy loop area, the more energy is required to break down the thixotropic structure, and the less sedimentation and the more stable for the paste [30]. Yield stress is an adscititious threshold shear stress for the whole paste to flow. It is defined as the intercepting point of two straight lines with different slopes where shear strain values are plotted versus shear stress [31]. The addition of fumed silica helped to improve the viscosity, thixotropy loop area and yield stress of the p-ICPC paste (Fig. 1; Table 1). In addition, the result showed a positive correlation between the yield stress values and thixotropy loop area of p-ICPC paste. The result indicated that the suspension stability of p-ICPC paste was enhanced with the increase of fumed silica concentration.

The injectability of biomaterial is affected by many factors [32, 33]. Although the injectability of p-ICPC was enhanced by PEG by reducing the friction coefficient, it

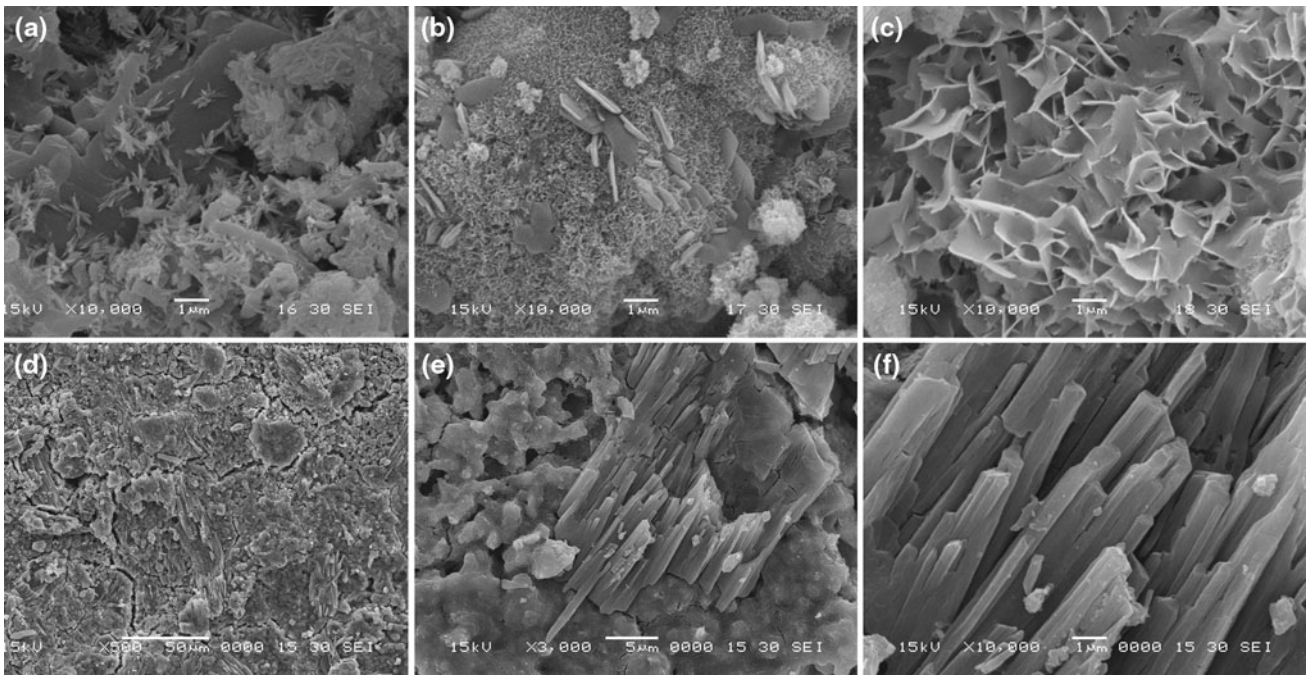

Fig. 6 SEM micrographs of fracture surface of hardened p-ICPC (1) after incubation in SBF for different times **a** 1 day (10000×), **b** 3 days (10000×), **c** 7 days (10000×), **d** 11 days (500×), **e** 11 days (3000×) and **f** 11 days(10000×)

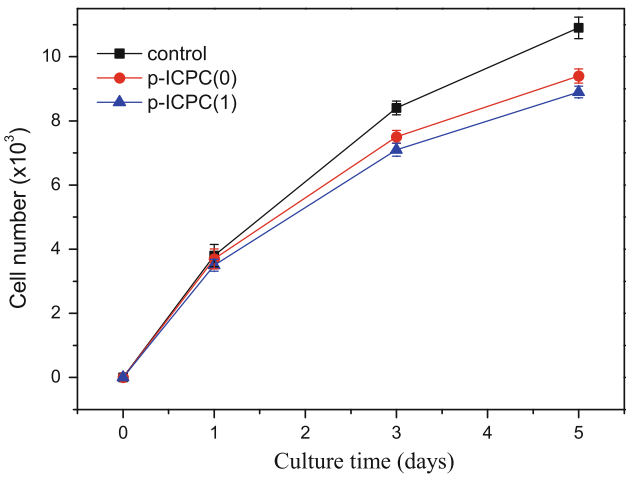

Fig. 7 Cell growth and proliferation of MG-63 cells cultured on the TCP control, p-ICPC (0) and p-ICPC (1) pastes at 1, 3 and 5 days of incubation

was decreased significantly with the increasing content of fumed silica (Fig. 2). The result accorded with the opinion that the larger the viscosity, the thixotropy area and the yield stress are, the more difficult the cement is to inject [34]. This phenomenon is due to the network structure formed by fumed silica, which directly resulted in higher stress at the outlet of the syringe and increased the initial injection pressure [35]. The addition of fumed silica does not decrease but increases the compressive strength of the paste slightly. This might be attributed to the reinforcement of fumed silica short fiber on the paste matrix. By comparison, p-ICPC (1) possesses good viscosity, extrudability and favorable suspension stability.

Although rheology determines the suspension stability indirectly, it can not provide information quantitatively about the actual behavior of the suspension. Without any dilution, Turbiscan LA-b$^{\text{Expert}}$ allows an early detection of slight changes in transmission and backscattering profiles before the appearance of a macroscopic scale sedimentation of the various concentrated dispersions [36]. The light transmittance reflects the paste stability while the backscattering light reflects the velocity of the particle sedimentation [37]. It should be pointed out that BS signal can only be analyzed if T signal is negligible. Otherwise, the partial reflection of the light crossing the sample by the walls of the measurement cell would interfere with the BS signal. In this study, the suspension stability of p-ICPC was performed on the Turbiscan LA-b $^{\text{Expert}}$, and p-ICPC (0) was used as a control.

After a period of storage, tiny particles tend to settle down to the bottom of the sample cell due to gravity, which leads to destabilization of the suspension. Interestingly, no sedimentation occurred in p-ICPC (1) at room temperature (Figs. 3, 4) even scanning for 10 days. Both T and BS in p-ICPC (1) remained close to zero all through the sample cell, even at the top. On the contrary, the p-ICPC (0) under the same condition stratified rapidly in two phases. The apparition of the nonaqueous phase was reflected by an increase in the T signals. Hence, the result confirmed that fumed silica helps to improve the stability of p-ICPC.

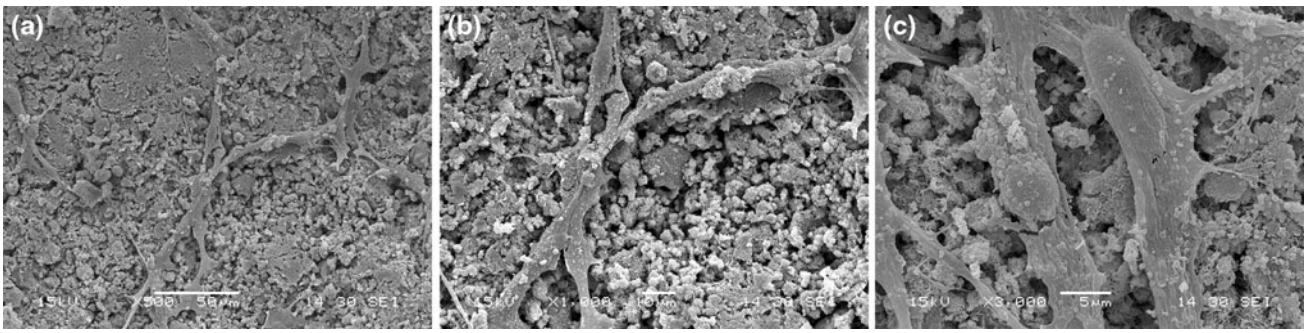

Fig. 8 SEM micrograph of MG-63 cells after culturing on the p-ICPC (1) for 3 days. **a** 500×, **b** 1000×, **c** 3000×

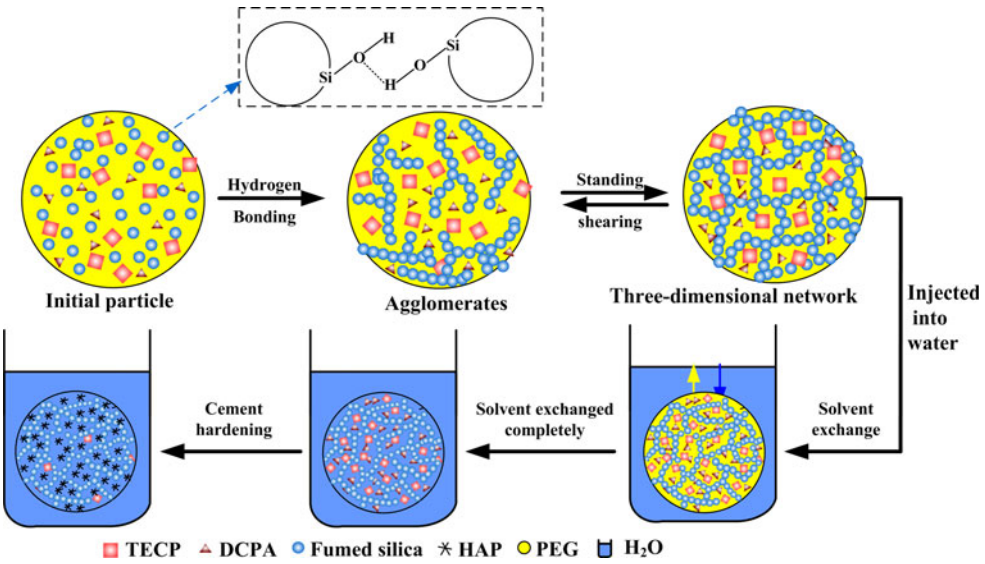

Fig. 9 Schematic representation of formation of fumed silica network in p-ICPC and the hydration of p-ICPC under aqueous circumstances

According to the Stokes' law (Eq. 1), the theoretical sedimentation rate is related to the viscosity: the higher the continuous phase viscosity, the lower the sedimentation velocity is. Fumed silica increased the viscosity of the pastes (Fig. 1a), and decreased the velocity of the particle sedimentation effectively, which was further verified by the stokes' law. In essence, the improvement on the suspension stability of p-ICPC is ascribed to the formation of 3D network of the fumed silica in PEG.

$$V_g = \frac{d^2(\rho_p - \rho_f)}{18\eta}\mu \quad (1)$$

where V_g is the sedimentation velocity (m s^{-1}); d is the particle diameter (m); ρ_p and ρ_f are the solid and continuous (oil) phases density (kg m^{-3}), respectively; η is the continuous phase viscosity; μ is the acceleration of centrifuge (m s^{-2}).

Based on the above analysis, we proposed the following model to elaborate the stability result of fumed silica as well as surface property, as shown in Fig. 9. In our study, fumed silica, with rich reactive hydroxyl groups on the surface [38], interacted with polar molecules PEG by the hydrogen bonding to form a 3D network. CPC particles are therefore trapped in the network. If the particles in the suspension are unstable, it has to overcome the "network powder" or the yield value. If the potential energy of particles is lower than the energy to destroy the network, the network structure will not be destroyed, thus the particles will be suspended in the liquid to stable the suspension. Kawaguchi et al. [39] considered the adsorption by the hydrogen bonding inhibited the aggregation of the silica particles effectively. Therefore, the network formed by fumed silica imparts the good dispersion to p-ICPC, not only increasing the viscosity but also inhibiting the sedimentation.

Figures 5a and 6 showed that p-ICPC (1) had been converted partially to needle-like HAP after soaking in SBF for 1d, although partial TECP and DCPA had not enough time to react to form HAP. With the further increase of immersion time, the conversion of p-ICPC (1) to HAP had more substantial increase. The morphology of the hydrated products changed from the needle, platelet to the rod-like. The relative intensity, number and size of HAP also increased with the immersion time. Therefore,

except the unique replacement between water and PEG, the hardening mechanism of p-ICPC is the same as that for aqueous CPC. Once p-ICPC was injected to physiological environment, the replacement occurred immediately between water and propylene glycol. With water penetrating into the p-ICPC gradually, TECP and DCPA were dissolved in the form of Ca^{2+}, PO_4^{3-} and OH^- ions, then reacted and reprecipitated to form HAP, as shown in Fig. 6. The rapid dissolution of Na_2HPO_4 increased the phosphate concentration effectively, thus accelerated the setting reaction of p-ICPC to form HAP [40]. Obviously, it was the replacement between water and PEG that prolonged the hydration process of p-ICPC.

The cytocompatibility was evaluated by monitoring the attachment and proliferation of MG-63 osteoblast-like cells cultured on the p-ICPC. The cell proliferation of p-ICPC (1) was not significantly different from p-ICPC (0). MG-63 cells attained normal spindle-like morphology and had developed with extensions adhering to the surface of the paste. The results suggested that p-ICPC (1) was cytocompatible. Among the constituents of p-ICPC (1), CPC has been proved to support cell attachment and proliferation because the individual components ($Ca_4(PO_4)_2O$, $CaHPO_4$) and the product of hydration (HAP) are biocompatible, which have been applied in clinic for many years [41–43]. In addition, PEG is known to be biocompatible and used in beverages, food, cosmetics and biomedical fields. Furthermore, fumed silica has been proved to be non-toxic in many fields [44, 45]. Therefore, from the composition point of view, it is not surprising that p-ICPC (1) would be compatible to the MG-63 cells in present study.

5 Conclusions

A premixed injectable calcium phosphate cement with excellent suspension stability was fabricated successfully by using fumed silica as a stabilizing agent and PEG as a nonaqueous phase. The suspension stability, rheological property, injectability, phase composition, microstructure and cytocompatibility in vitro of p-ICPC were systematically investigated. Although fumed silica decreased the injectability of p-ICPC, the addition of fumed silica improved the compressive strength and suspension stability of the p-ICPC prominently, and had no influence on the conversion to HAP under aqueous circumstances. The results showed that p-CPC (1) not only possesses proper thixotropy, compressive strength and injectability but has good cytocompatibility as well. It was noteworthy that p-ICPC (1) had a potent suspension stability observed by rheometer and Turbiscan LA-b^{Expert}. These observations may have applicability to develop other nonaqueous injectable biomaterials for non-immediate filling and long-term storage.

Acknowledgments This investigation was supported by the National Basic Research Program of China (973 Program: 2012CB933600, 2012BAD32B01), National Natural Science Foundation of China (31100678, 31271010), Natural Science Foundation of Shanghai City (11ZR1408200), Fundamental Research Funds for the Central Universities (WD1114048) and Program of Shanghai Leading Academic Discipline Project (No. B502). We also greatly thank Professor Gregory F.Payne of university of Maryland for his English modification.

References

1. Ambrosio L, Guarino V, Sanginario V, Torricelli P, Fini M, Ginebra MP, et al. Injectable calcium–phosphate-based composites for skeletal bone treatments, Biomedical Mater. (2012);7. doi: 10.1088/1748-6041/7/2/024113.
2. Friedman CD, Costantino PD, Takagi S, Chow LC. BoneSource™ hydroxyapatite cement: a novel biomaterial for craniofacial skeletal tissue engineering and reconstruction. J Biomed Mater Res: Appl Biomater. 1998;43:428–32.
3. Chow LC. Calcium phosphate cements: chemistry, properties, and applications. Mater Res Symp Proc. 2000;599:27–37.
4. Xu HHK, Careya LE, Takagi S, Chow LC. Premixed calcium phosphate cements: synthesis, physical properties, and cell cytotoxicity. Dent Mater. 2007;23:433–41.
5. Takagi S, Chow LC, Hirayama S, Sugawara A. Premixed calcium phosphate cement pastes. J Biomed Mater Res. 2003;67B: 689–96.
6. Wei J, Li YB. Injectable premixed cement of nanoapatite and polyamide composite. High Technol Lett. 2002;2:18–22.
7. Uwe G, Sofia D, Roger T, Jake EB. Factors influencing calcium phosphate cement shelf-life. Biomaterials. 2005;26:3691–7.
8. Chow LC, Hirayanma S, Takagi S, Parry E. Diametral tensile strength and compressive strength of a calcium phosphate cement: effect of applied pressure. J Biomed Mater Res: Appl Biomater. 2000;53:511–7.
9. Lisa E, Xu HHK, Careya CG, Simon J, Takagia S, Chow LC. Premixed rapid-setting calcium phosphate composites for bone repair. Biomaterials. 2005;26:5002–14.
10. Trammer B, Amann A, Haltner-Ukomadu E, Tillmanns S, Keller M, Hogger P. Comparative permeability and diffusion kinetics of cyclosporine a liposomes and propylene glycol solution from human lung tissue into human blood ex vivo. Euro J Pharm Biopharm. 2008;70:758–64.
11. Fine A, Patterson J. Severe hyperphosphatemia following phosphate administration for bowel preparation in patients with renal failure: two cases and a review of the literature. Am J Kidney Dis. 1997;29:103–5.
12. Harris J. Introduction to biotechnical and biomedical applications of poly (ethylene glycol). New York: Chemistry Plenum Press; 1992.
13. Xu HHK, Takagi S, Quinn J, Chow LC. Fast-setting calcium phosphate scaffolds with tailored macropore formation rates for bone regeneration. J Biomed Mater Res. 2004;68A:725–34.
14. Briak HE, Durand D, Nurit J, Munier S, Pauvert B, Boudeville P. Study of a hydraulic dicalcium phosphate dihydrate/calcium oxide-based cement for dental applications. J Biomed Mater Res. 2002;63:447–53.
15. Ettlinger M, Ladwig T, Weise A. Surface modified fumed silicas for modern coatings. Prog Org Coat. 2000;40:31–4.
16. Chung SJ, Leonard JP, Nettleship I, Lee JK, Soong Y, Martello DV. Characterization of ZnO nanoparticle suspension in water:

effectiveness of ultrasonic dispersion. Powder Technol. 2009;194: 75–80.
17. Ciftci D, Kahyaoglu T, Kapucu S, Kaya S. Colloidal stability and rheological properties of sesame paste. J Food Eng. 2008;87: 428–35.
18. Hugo Leonardo RA, Luis AS, Carlos PB. Injectability evaluation of tricalcium phosphate bone cement. J Mater Sci Mater Med. 2008;19:2241–6.
19. Burguera EF, Xu HHK, Sun L. Injectable calcium phosphate cement: effects of powder-to-liquid ratio and needle size. J Biomed Mater Res. 2008;84B:493–502.
20. http://www.turbiscan.com/home/lab_present1.htm.
21. Kokubo T, Takadama H. How useful is SBF in predicting in vivo bone bioactivity? Biomaterials. 2006;27:2907–15.
22. Rankin PJ, Horvath AT, Klingenberg DJ. Magnetorheology in viscoplastic media. Rheol Acta. 1999;38:471–7.
23. Chen FP, Liu CS, Wei J, Mao YH. Preparation and characterization of injectable calcium phosphate cement paste modified by polyethylene glycol-6000. Material Chemical and Physic. 2011;125: 818–24.
24. Bossis G, Volkova O, Lacis S, Meunier A. In: Odenbach S (Ed.) Ferrofluids, Chap. 11. Berlin: Springer; 2002.
25. de Vicente J, Lopez–Lopez MT, Gonzalez-Caballero F, Duran JDG. Rheological study of the stabilization of magnetizable colloidal suspensions by addition of silica nanoparticles. J Rheol. 2003;47:1093–109.
26. Volkova O, Bossis G, Guyot M, Bashtovoi V, Reks A. Magnetorheology of magnetic holes compared to magnetic particles. J Rheol. 2000;44:91–104.
27. Asai H, Masuda A, Kawaguchi M. Rheological properties of colloidal gels formed from fumed silica suspensions in the presence of cationic surfactants. J Colloid Interface Sci. 2008;328:180–5.
28. Wang XP, Chen L, Xiang H, Ye JD. Influence of anti-washout agents on the rheological properties and injectability of a calcium phosphate cement. J Biomed Mater Res. 2007;81B:410–8.
29. Mewis J, Wagner NJ. Thixotropy. Adv Colloid Interface Sci. 2008;147:214–27.
30. Liu CS, Shao HF, Chen FY, Zheng HY. Rheological properties of concentrated aqueous injectable calcium phosphate cement slurry. Biomaterials. 2006;27:5003–13.
31. Joao B, Neto R, Moreno R. Effect of mechanical activation on the rheology and casting performance of kaolin/talcalumina suspensions for manufacturing dense cordierite bodies. Appl Clay Sci. 2008;38:209–18.
32. Qi XP, Ye JD, Wang YJ. Improved injectability and in vitro degradation of a calcium phosphate cement containing poly(lactide-*co*-glycolide) microspheres. Acta Biomater. 2008;4:1837–45.
33. Leroux L, Hatim Z, Freche M, Lacout JL. Effects of various adjuvants (lactic acid, glycerol, and chitosan) on the injectability of a calcium phosphate cement. Bone. 1999;25:31S–4S.
34. Chen FP, Mao YH, Liu CS. Bismuth-doped injectable calcium phosphate cement with improved radiopacity and potent antimicrobial activity for root canal filling. Acta Biomater. 2010;6: 3199–207.
35. Bohner M, Baroud G. Injectability of calcium phosphate pastes. Biomaterials. 2005;26:1553–63.
36. Mengual O, Meunier G, Cayre I, Puech K, Snabre P. Characterisation of instability of concentrated dispersions by a new optical analyser: the Turbiscan MA 1000 Colloids Surf. A: Physicochem. Eng. Aspects. 1999;152:111–23.
37. Kim HS, Park WI, Kang M, Jin HJ. Multiple light scattering measurement and stability analysis of aqueous carbon nanotube dispersions. J Phys Chem Solid. 2009;69:1209–12.
38. Raghavan S, Walls HJ, Khan SA. Rheology of silica dispersions in organic liquids: new evidence for solvation forces dictated by hydrogen bonding. Langmuir. 2000;16:7920–30.
39. Kawaguchi M, Yamamoto T, Kato T. Rheological properties of silica suspensions in aqueous solutions of block copolymers and their water-soluble components. J Colloid Interface Sci. 2001;241: 293–5.
40. Onuma K. Recent research on pseudobiological hydroxyapatite crystal growth and phase transition mechanisms. Progr Cryst Growth Char Mater. 2006;52:223–45.
41. Knabe C, Berger G, Gildenhaar R, Meyer J. Howlett CR, Markovic B, Effect of rapidly resorbable calcium phosphates and a calcium phosphate bone cement on the expression of bone-related genes and proteins in vitro. J Biomed Mater Res. 2004;69A:145–54.
42. Ehara A, Ogata K, Imazato S, Ebisu S, Nakano T, Umakoshi Y. Effects of alpha-TCP and TetCP on MC3T3-E1 proliferation, differentiation and mineralization. Biomaterials. 2003;24:831–6.
43. Yuasa T, Miyamoto Y, Ishikawa K, Takechi M, Momota Y, Tatehara S. Effects of apatite cements on proliferation and differentiation of human osteoblasts in vitro. Biomaterials. 2004;25: 1159–66.
44. Jia H, Hou W, Wei L, Xu B, Liu X. The structures and antibacterial properties of nano-SiO_2 supported silver/zinc-silver materials. Dent Mater. 2008;24:244–9.
45. Slowing II, Vivero-Escoto JL, Wu CW, Lin VSY. Mesoporous silica nanoparticles as controlled release drug delivery and gene transfection carriers. Adv Drug Delivery Rev. 2008;60:1278–88.